

QCD Analysis of Dijet Production at Low Q^2 at HERA

J. Chýla, J. Cvach, K. Sedlák, M. Taševský

Abstract

Recent H1 data on triple differential dijet cross sections in $e^\pm p$ interactions in the region of low photon virtualities are shown to be in reasonable agreement with the predictions of the NLO QCD calculations obtained using the program NLOJET++. The implications of this observation for the phenomenological relevance of the concept of resolved virtual photon are discussed.

1 Introduction

Recent H1 data on triple differential dijet cross sections in $e^\pm p$ interactions in the region of low photon virtualities [1] have revealed a clear excess of the data over NLO QCD predictions obtained using the DISENT program [2]. This excess comes predominately from the region of low photon virtualities Q^2 ($Q^2 \gtrsim 2 \text{ GeV}^2$) and small x_γ ($x_\gamma \leq 0.75$), where x_γ denotes fraction of the four-momentum of the photon carried by the parton involved in the hard collision¹. We recall that DISENT dispenses with the concept of resolved photon and evaluates, up the order $\alpha\alpha_s^2$, the direct photon contribution only. In the region $Q^2 \gtrsim 2 \text{ GeV}^2$ this is quite a legitimate procedure. However, it has been argued [3, 4] that even for such moderate values of Q^2 the concept of resolved virtual photon is useful phenomenologically as a way of resumming part of higher order direct photon contributions. These higher order QCD corrections are important particularly in the region $x_\gamma \leq 0.75$, to which only the lowest order tree level diagrams contribute in DISENT.

In this region DISENT calculations are described by diagrams exemplified by those in Fig. 1a,c. In the kinematic region $\tau_1 \ll \tau_2 \simeq E_T^2$ (where τ_1, τ_2 denote the virtualities of the ladder partons in Fig. 1a,c) the contribution to the dijet cross section coming from the diagram in Fig. 1a can be approximated by the sum of the convolutions which describe the contributions of transverse ($k = T$) and longitudinal ($k = L$) polarizations of the virtual photon.

$$\frac{d\sigma_k(ep \rightarrow jets)}{dydQ^2dx_\gamma dE_T^2} \propto f_{\gamma/e}(y, Q^2) \otimes D_{q/\gamma_k^*}^{\text{QED}}(x_\gamma, Q^2, E_T^2) \otimes \frac{d\sigma^{LO}(q\bar{q} \rightarrow GG; yx_\gamma)}{dE_T^2} \quad (1)$$

where

$$f_T(y, Q^2) = \frac{\alpha}{2\pi} \left[\frac{2(1-y) + y^2}{y} \frac{1}{Q^2} - \frac{2m_e^2 y}{Q^4} \right], \quad (2)$$

$$f_L(y, Q^2) = \frac{\alpha}{2\pi} \left[\frac{2(1-y)}{y} \frac{1}{Q^2} \right]. \quad (3)$$

describe the fluxes of transverse and longitudinal photons in the incoming electron, the QED contributions to the quark and gluon distribution functions of the transverse and longitudinal virtual photons are given as

$$D_{q_i/\gamma_T^*}^{\text{QED}}(x_\gamma, Q^2, M^2) = \frac{\alpha}{2\pi} 3e_i^2 (x_\gamma^2 + (1-x_\gamma)^2) \ln \frac{M^2}{x_\gamma Q^2}, \quad (4)$$

$$D_{q_i/\gamma_L^*}^{\text{QED}}(x_\gamma, Q^2, M^2) = \frac{\alpha}{2\pi} 3e_i^2 4x_\gamma(1-x_\gamma) \left(1 - \frac{x_\gamma Q^2}{M^2} \right), \quad (5)$$

$$D_{G/\gamma_{T,L}^*}^{\text{QED}}(x_\gamma, Q^2, M^2) = 0, \quad (6)$$

and $\sigma^{LO}(q\bar{q} \rightarrow GG)$ stands for the lowest order contribution to the cross section of the process $q\bar{q} \rightarrow GG$. Similar expressions can be written for other partonic subprocesses. In Eqs. (4-6), e_i denotes the electric charge of the quark q_i and M stands for the factorization scale, in (1) identified with jet transverse energy. The full expressions for the distribution functions (4-6), containing the exact Q^2 dependence with the correct threshold behaviour for $Q^2/m_q^2 \rightarrow 0$, can be found in [4]. The contributions of the diagrams in Fig. 1a,c contain also singularities coming from the region of small τ_2 and those of Fig. 1b,d from the region of small τ_3 , but these are understood to be absorbed in the parton distribution functions of the proton.

¹We use the notation and terminology as described in detail in [1].

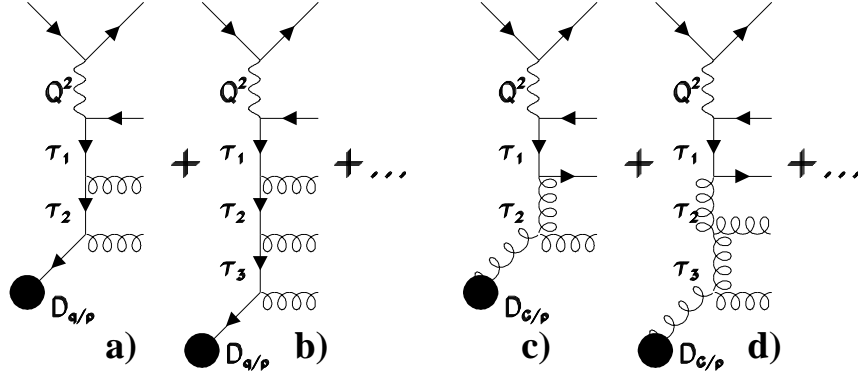


Figure 1: Examples of the LO (a) and (c) and NLO (b) and (d) Feynman diagrams included in NLOJET++ and contributing to the three jet cross section in the region $x_\gamma \leq 0.75$. In the framework of the concept of resolved virtual photon the integrals over the region of small τ_1 give rise to quark (a-c) and gluon (d) distribution function of the photon.

In [1] it has also been shown that adding in HERWIG the LO resolved photon contribution to the LO direct one helps bring the QCD predictions closer to the data. At the NLO such a procedure can be performed only at the parton level and currently only within the JETVIP program [5]. The NLO QCD corrections come loop corrections to LO diagrams like those of Fig. 1a,c and from tree Feynman diagrams exemplified by those of Fig. 1b,d, which contain terms proportional to the "large collinear logs" of the form $\ln^2(E_T^2/\tau_2)$. Within the framework of resolved virtual photon contribution, these terms can be interpreted as lowest QCD corrections to the purely QED part of quark and gluon distribution functions of the photon (4-5). In Fig. 2 they correspond to the second (first) term in the definition of the so called pointlike part of quark (gluon) distribution function $D_{q/\gamma}^{\text{PL}}$ ($D_{G/\gamma}^{\text{PL}}$) of the photon [3].

Contrary to DISENT, which uses the subtraction method, JETVIP employs the phase space slicing method to regularize mass singularities. Unfortunately, the NLO resolved photon calculations obtained with JETVIP turned out [6] to be rather sensitive to choice the associated slicing parameter y_c . Consequently, although adding resolved photon contribution worked in the right direction, no quantitative conclusion could be drawn [1].

The situation has recently changed due to the appearance of the NLOJET++ program [7], which allows the user to calculate beside single and dijet cross sections also the triple jet cross sections to the NLO. This program uses the same subtraction method as DISENT and similarly as the latter dispenses with the concept of resolved virtual photon. As far as single and double jet cross sections are concerned it is thus in principle identical to DISENT. It, however, provides also the option – which we shall call 3-jet mode – of calculating NLO QCD correction to three well separated jets. This mode can be selected by cutting off the region of x_γ close to 1, where also the dijet final states contribute. Respecting the binning of the data in [1] we set $x_\gamma \leq 0.75$. Comparing the results obtained with NLOJET++ and JETVIP we could address two questions:

- how important are terms of the order $\alpha\alpha_s^3$ included in exact NLO calculations,
- how important is the all order resummation of the collinear logarithms into the QCD-improved PDF of the photon used in the resolved photon contribution of JETVIP?

Unfortunately, as mentioned above the NLO resolved photon contribution are rather sensitive to the variation of the slicing parameter y_c . Moreover, there is also a sizable discrepancy between

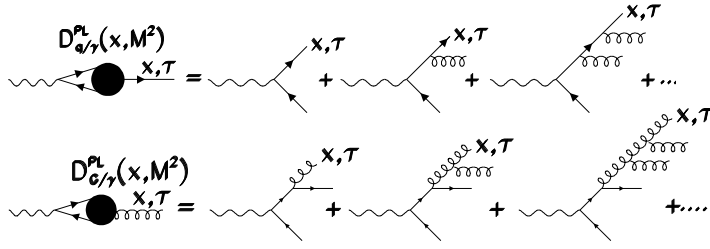


Figure 2: Graphs contributing to the definition of the pointlike part of quark and gluon distribution functions of the photon.

the results of the NLO direct photon contribution of JETVIP on one side and those of DISENT or NLOJET++ in 2-jet mode on the other, with JETVIP results lying in the region $x_\gamma \leq 0.75$ significantly below those of DISENT or NLOJET++. This discrepancy, clearly visible in Fig. 3, is not understood.

2 Data Selection

The data employed in this article have been published in [1], where a detailed description of event selection and experimental methods used in their extraction can be found. Only the main facts are therefore recalled. The data, taken at HERA in the years 1999 and 2000, when electrons with an energy of 27.55 GeV collided with protons with an energy of 920 GeV, correspond to an integrated luminosity of 57 pb^{-1} . The kinematic region of the present analysis is defined by cuts on the photon virtuality Q^2 and its inelasticity y

$$2 < Q^2 < 80 \text{ GeV}^2, \quad 0.1 < y < 0.85 \quad (7)$$

as well as by cuts on the hadronic final state, which has to contain at least two jets found using the longitudinally invariant k_t jet algorithm [8]. The jet transverse energies, E_T^* , and pseudorapidities, η^* , are calculated relative to the γ^*p collision axis in the γ^*p center-of-mass frame. The jets are ordered according to their transverse energy, with jet 1 being the highest E_T^* jet. The two jets with the highest transverse energies (leading jets) are required to satisfy

$$E_{T1}^* > 7 \text{ GeV}, \quad E_{T2}^* > 5 \text{ GeV}, \quad (8)$$

$$-2.5 < \eta_1^* < 0, \quad -2.5 < \eta_2^* < 0. \quad (9)$$

In total 105 658 events satisfied these selection criteria. For dijet events the variable

$$x_\gamma^{\text{jets}} = \frac{\sum_{j=1,2} (E_j^* - p_{z,j}^*)}{\sum_{\text{hadrons}} (E^* - p_z^*)} \quad (10)$$

was used as a hadron level estimate of x_γ . The sum in the numerator runs over the two leading jets and the sum in the denominator includes the full hadronic final state.

The data were corrected for initial and final state QED radiation effects, trigger inefficiencies, limited detector acceptance and resolution and a photoproduction background. The systematic errors of different origin are added in quadrature. The dominant source of the systematic error arises from the uncertainty of the energy calibration of the H1 calorimeters and the model dependence of acceptance corrections [1].

3 Results

In Fig. 3 the NLOJET++ results corresponding to both 2-jet and 3-jet modes and evaluated in the kinematic region (7-9) are compared with the H1 data [1]. For comparison, the results obtained with DISENT [1] are plotted as well.

There is a large difference between the NLOJET++ results obtained in 2-jet and 3-jet modes, the latter lying systematically above the former. This difference, which is most pronounced for small x_γ and low Q^2 , indicates the importance of the NLO QCD corrections in this region. The NLOJET++ results in the 3-jet mode come significantly closer to the data than those of the 2-jet mode, but they still undershoot it. The remaining gap between the data and NLOJET++ calculations in the 3-jet mode is again most pronounced for small x_γ and low Q^2 . In view of large NLO QCD corrections in this region this remaining discrepancy is not surprising and allows room for still higher order QCD corrections.

At the moment the only, though approximate, way of estimating these higher order terms exploits the concept of resolved virtual photon and the only code that offers this option at the NLO is JETVIP. Despite the problems mentioned above, we plot in Fig. 3 the full JETVIP results [1], i.e. the sum of direct (with photon splitting term subtracted) and resolved photon contributions. Ideally, one would expect the full JETVIP results to be above those of NLOJET++ in 3-jet mode. Fig. 3 shows that they are in fact close to each other. This may be caused by various effects, but we would like to point out the following one. As already mentioned above the direct photon results of JETVIP are systematically below those of NLOJET++ in the two jet mode. Assuming the latter are correct but the resolved photon contribution is estimated correctly by JETVIP, the "correct" full JETVIP should lie somewhat above the NLOJET++ 3-jet mode predictions and close to the data. At the moment, this is just a pure speculation, but we hope to check it, once a new version of JETVIP becomes available [9].

In summary, we have shown that the NLOJET++ calculations of the dijet cross sections in the 3-jet mode are significantly closer to the H1 data [1] than those of DISENT. This demonstrates the importance of the NLO QCD corrections in processes involving virtual photons. The remaining gap between the data and current QCD calculations in the region of low Q^2 and small x_γ may be closed using the concept of the resolved virtual photon contribution.

Acknowledgements

We are grateful to Z. Nagy and Z. Trócsányi for extensive correspondence on some aspects of using their code, to R. Pöschl for help in running the NLOJET++ code and to Tancredi Carli for drawing our attention to the 3-jet mode of NLOJET++. This work has been supported by the Ministry of Education of the Czech Republic under the project LN00A006.

References

- [1] A. Aktas *et al.* [H1 Collaboration], Eur. Phys. J. C **37** (2004) 141 [hep-ex/0401010].
- [2] S. Catani, M. Seymour, Nucl. Phys. **B 485** (1997), 291
- [3] G. A. Schuler and T. Sjöstrand, Phys. Lett. B **376** (1996) 193 hep-ph/9601282,
M. Glück, E. Reya and M. Stratmann, Phys. Rev. **D 54** (1996) 5515 hep-ph/9605297.
M. Glück, E. Reya and I. Schienbein, Phys. Rev. **D 60** (1999) 054019, hep-ph/9903337.

- [4] J. Chýla and M. Taševský, Phys. Rev. D **62** (2000) 114025 hep-ph/9912514.
 [5] B. Pötter, Comput. Phys. Commun. **119** (1999) 45, **133** (2000) 105.
 [6] K. Sedlak, PhD Thesis, Prague, June 2004
 [7] Z. Nagy, Z. Trócsányi, Phys. Rev. Lett. **87** (2001), 082001
 [8] S. Catani, Y. L. Dokshitzer, M. H. Seymour, B. R. Webber, Nucl. Phys. B **406** (1993) 187.
 [9] M. Klasen, private communication

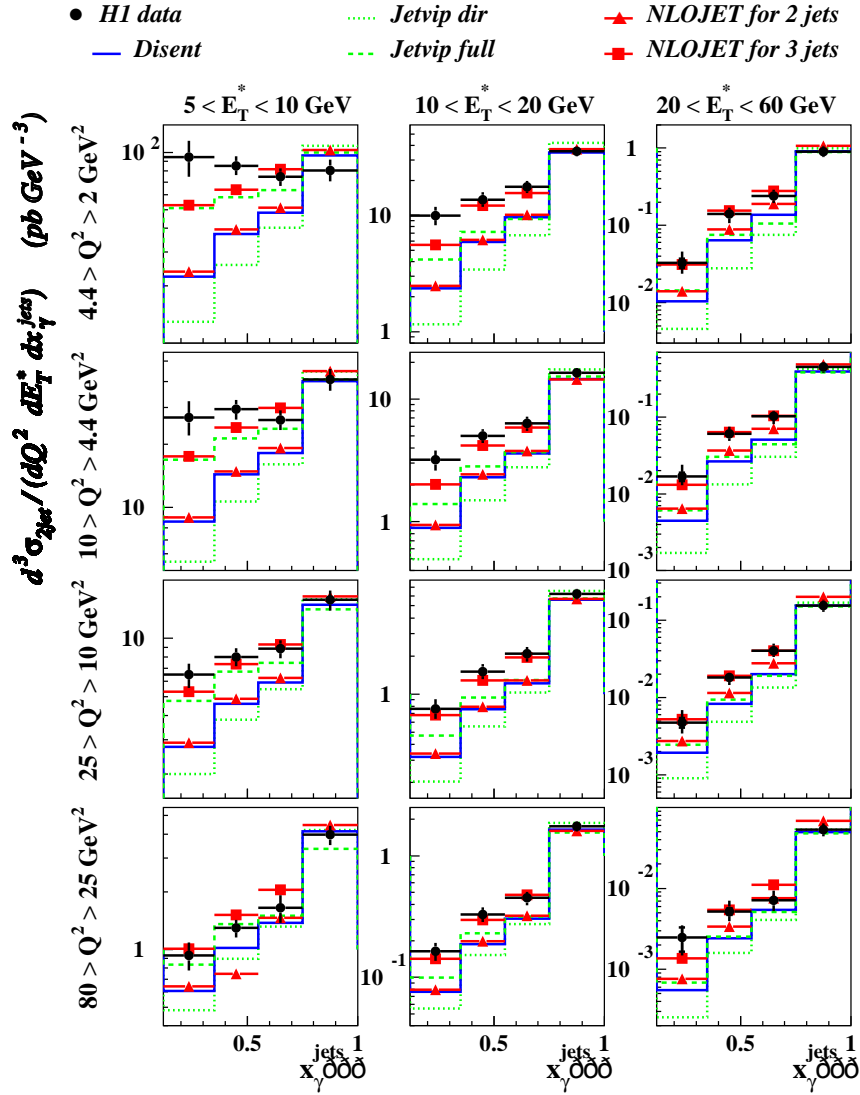


Figure 3: Triple differential dijet cross section $d^3\sigma_{2\text{jet}}/dQ^2 dE_T^* dx_\gamma^{\text{jets}}$ with asymmetric E_T^* cuts (see text). The inner error bars on the data points show the statistical error, the outer ones the quadratic sum of systematic and statistical errors. The data are compared to NLO direct photon calculations using DISENT (full line) and JETVIP (dotted line), the sum of NLO direct and resolved photon contributions of JETVIP (dashed line) and the NLOJET++ predictions in 2-jet (triangles) and 3-jet (squares) mode. All calculations are corrected for hadronisation effects.